

# Volum e D ependence of the P ion M ass in the Q uark-M eson-M odel

J. Braun,<sup>1</sup> B. Klein,<sup>1</sup> and H. J. Pirner<sup>1,2</sup>

<sup>1</sup>Institute for Theoretical Physics, University of Heidelberg, Philosophenweg 19, 69120 Heidelberg

<sup>2</sup>Max-Planck-Institut für Kernphysik, Saupfercheckweg 1, 69117 Heidelberg

(D ated: February 8, 2020)

We consider the quark-meson-m odel in a nite three-dimensional volum e using the Schwinger propertim e renormalization group. We derive and solve the ow equations for nite volum e in local potential approximation. In order to break chiral symmetry in the nite volum e, we introduce a small current quark mass. The corresponding effective meson potential breaks chiral O(4) symmetry explicitly, depending on and  $\sim$  elds separately. We calculate the volum e dependence of the pion mass and of the pion decay constant with the renormalization group ow equations and compare with recent results from chiral perturbation theory in a nite volum e.

## I. INTRODUCTION

The study of QCD in a nite volum e has been of interest for quite some time. Accurate results of lattice simulations with dynamical fermions necessitate understanding nite volum e effects. A variety of different methods has been proposed, cf. refs. [1, 2, 3, 4, 5, 6, 7, 8, 9], to extrapolate reliably from nite lattice volumes to the infinite volume. Finite volume partition functions for QCD have attracted interest in their own right, because they allow an exact description of QCD at low energies [10, 11, 12, 13]. The low energy behavior of QCD is determined by spontaneous chiral symmetry breaking [14], which, however, does not occur in a nite volume. If the current quark mass is set equal to zero, in a nite volume the expectation value for the order parameter of chiral symmetry breaking vanishes, remaining zero even for arbitrary large volumes. The order parameter has a nite expectation value only when the infinite volume limit is taken before the quark mass is set to zero.

The box size  $L$ , the pion mass  $m$  and the pion decay constant  $f$  are the relevant scales for the transition between the regimes with a strongly broken and with an effectively restored chiral symmetry [10]. As a measure of explicit symmetry breaking, the pion mass is of particular importance. It is primarily the dimensionless product  $m/L$  that determines in

which regime the system exists for a given pion mass and volume. In order to study chiral symmetry breaking in a finite volume, it is essential to introduce a finite quark mass as a parameter that explicitly breaks the chiral symmetry. Such an explicit symmetry breaking is quite natural in theories which involve effective chiral Lagrangians.

QCD at low energy can be studied by a wide variety of approaches which in essence all rely on the same fact: Due to spontaneous breaking of chiral symmetry, low-energy QCD is dominated by massless Goldstone bosons associated with the broken symmetry. Since these Goldstone bosons interact only weakly, the low-energy limit of QCD can be described in terms of an effective theory of these fields. A description in terms of effective chiral Lagrangians becomes even better if one considers the partition functions in finite Euclidean volume. Compared to the light degrees of freedom, contributions of heavier particles are suppressed by  $e^{-M L}$ , where  $M$  is the typical separation of the hadronic mass scale from the Goldstone masses. This separation of mass scales is at the origin of the description of QCD with effective theories in terms of the light degrees of freedom only.

Groundbreaking work has been done by Gasser and Leutwyler [10, 11, 12] in chiral perturbation theory, and by Leutwyler and Smilga for the eigenvalue spectrum of the QCD Dirac operator [13]. Random matrix theory [15, 16] predicts analytically the volume and quark mass dependence of the chiral condensate [17, 18, 19], and the eigenvalue spectrum which has been well confirmed by numerous lattice results, see e.g. [19, 20, 21]. Such analytic predictions have been extremely useful as a check for calculations in lattice gauge theory.

In the context of the renormalization group (RG) approach, most calculations so far have been done in a chirally symmetric formulation [22, 23, 24, 25]. In such a framework, explicit symmetry breaking terms do not affect the renormalization group flow. This means that pion contributions to the renormalization group flow come from exactly massless pions. Small quark masses can be converted into a small linear term in the meson potential which is not renormalized and can therefore be added at the end of the evolution. In this paper, we will present a formulation which includes explicit symmetry breaking in the renormalization group flow and which can be used also for a finite volume.

We use the chiral quark-meson model, which contains a scalar sigma meson and quarks in addition to the pion degrees of freedom. It is well known that the linear sigma model alone is not compatible with the low energy scattering data [14]. Due to the presence of quarks, the low energy constants of chiral perturbation theory are reproduced [26, 27].

The quark-meson model is evolved with renormalization group flow equations which connect different scales. As we will demonstrate, the inverse box size  $1=L$  acts as an effective cut-off scale which freezes the evolution when the evolution parameter  $k < =L$ . In the same way as the renormalization group flow equations describe the dependence of the results on the renormalization cut-off scale  $k$ , they also describe the dependence on the additional scale imposed by the finite volume. The summation of higher loop graphs in this approach does allow to extend the calculation to smaller quark masses and volumes, where perturbative calculations lack convergence. Deviations of the calculated pion mass correction in the finite volume from chiral perturbation theory are found in this region. Our results agree, however, in the case of large pion masses and large volumes.

The paper is organized as follows: In section II, we review recent results from the application of chiral perturbation theory to the problem of finite volume effects. In section III, we show how the evolution equation for the effective meson potential is modified in a finite volume. Details of the numerical evaluation are discussed in section IV. In section V we present our final results, which are discussed in section VI.

## II. FINITE VOLUME EFFECTS IN CHIRAL PERTURBATION THEORY

For finite volume, massless Goldstone bosons dominate the action of a theory with broken chiral symmetry. In chiral perturbation theory (chPT) [14], the pion mass, the pion decay constant and the chiral condensate have been calculated [10, 11, 12]. The expansion parameters are the magnitude of the three-momentum  $p_j$  and the mass of the pion  $m$  as the lightest degree of freedom compared with the chiral symmetry breaking scale  $4\pi f$ .

Depending on the size  $L$  of the volume and the pion mass  $m$ , chiral perturbation theory distinguishes between two different power counting schemes. If the size of the box is much larger than the Compton wavelength of the pion  $L \gg 1/m$ , the lowest nonzero pion momentum is smaller than the pion mass ( $p_{\text{min}} = \frac{2\pi}{L} \ll m$ ) and the normal power counting scheme applies ("p-regime"). In this case, the pions are constrained very little by the presence of the box, and finite size effects are comparatively small [12]. If, on the other hand, the size of the box is smaller than the Compton wavelength of the pion, the normal chiral expansion breaks down, since the smallest momentum  $p_{\text{min}} = \frac{2\pi}{L} \gg m$  is now much larger than the pion mass ("v-regime"). In this case, the partition function is dominated by the

zero mass modes. After solving the zero-mass momentum sector of the theory exactly, one expands the finite mass momentum modes to one-loop order.

A very useful tool to study the effects of a finite volume on the mass of the pion is Luscher's formula [28]. It relates the leading finite volume corrections for the pion mass in Euclidean volume to the  $\pi$ -scattering amplitude in finite volume. Corrections to the leading order behavior drop at the least as  $O(e^{mL})$  where  $m = \frac{p}{3=2m}$ . For the particular case of the pion mass, the formula for the relative deviation  $R[m(L)]$  of the pion mass  $m(L)$  in the finite volume from the pion mass in the infinite volume  $m(1)$  reads as follows:

$$R[m(L)] = \frac{m(L) - m(1)}{m(1)} = \frac{3}{16^2 m} \frac{1}{m} \frac{1}{L} \int_1^{\infty} dy F(iy) e^{-\frac{p}{m^2 + y^2} L} + O(e^{mL}): \quad (1)$$

$F$  is the forward  $\pi$ -scattering amplitude as a function of the energy variable  $s$  continued to complex values. New results [8, 9] have recently been obtained by combining Luscher's formula with a calculation of the scattering amplitude in chiral perturbation theory. A next-to-next-to leading order calculation of  $F$  alone does not seem to give a reliable and satisfactory result. A one-loop calculation using Luscher's formula gives a shift in the pion mass, for example, which is substantially lower than the one expected from the full one-loop calculation in chiral perturbation theory as performed by Gasser and Leutwyler [11]. This estimate of the finite volume effects can be improved, if one uses the mass correction obtained from Luscher's formula with a  $\pi$ -scattering amplitude including higher orders to correct the full one-loop chiral perturbation theory result [9]. Since Luscher's formula has sub-leading corrections  $O(\exp[-\frac{p}{3=2m} L])$ , the corrections to the leading result increase for decreasing pion mass at fixed volume size  $L$  with  $m \ll L$ . As pointed out by the authors in [9], the Luscher formula becomes a less reliable approximation exactly for those values of the pion mass for which the chiral expansion converges especially well.

The renormalization group flow equations do not rely on either box size or pion mass as an expansion parameter, and do not require to distinguish between two different regimes. They remain valid as long as the lowest momenta and the masses of the heaviest particles remain below the ultraviolet cut-off scale  $u_v = 1.5$  GeV. The beauty of the renormalization group method is precisely that the flow equations connect different scales. In the same way as the renormalization group flow equations describe the dependence of the results on the infrared cut-off scale  $k$ , they also describe the dependence on the additional scale imposed

by the finite volume.

### III. RENORMALIZATION GROUP FLOW EQUATIONS FOR THE QUARK-MESON-MODEL

The quark-meson model is an  $SU(2)_L \times SU(2)_R$  invariant linear model with chiral mesons  $\pi^0, \pi^+, \pi^-$  coupled to constituent quarks  $q, \bar{q}$ . It is an effective model for dynamical spontaneous chiral symmetry breaking at intermediate scales of  $k \sim \mu_{UV}$ , where the ultra-violet scale  $\mu_{UV} \sim 1.5$  GeV is determined by the validity of a hadronic representation of QCD. At the UV scale  $\mu_{UV}$ , the quark-meson model is defined by the effective Lagrangian

$$Z_{UV}[\phi, q, \bar{q}] = \int d^4x \left[ \bar{q} \not{\partial} q + \bar{q} q (\frac{1}{2} \partial_\mu \phi \partial^\mu \phi + \frac{1}{2} m_c^2 \bar{q} q) + U(\phi) \right] \quad (2)$$

in a four-dimensional Euclidean volume with compact Euclidean time direction. The partition function  $Z$  has the path integral representation

$$Z = \int D\phi Dq D\bar{q} \exp(-S_{UV}) \quad (3)$$

where in the Euclidean time direction periodic and anti-periodic boundary conditions apply for bosons and fermions, respectively. A Gaussian approximation to the path integral followed by a Legendre transformation yields the 1-loop effective action for the scalar fields

$$S_{UV}[\phi] = S_{0,UV}[\phi] - \text{Tr} \log \Gamma_F^{(2)}[\phi] + \frac{1}{2} \text{Tr} \log \Gamma_B^{(2)}[\phi] \quad (4)$$

where  $\Gamma_B^{(2)}[\phi]$  and  $\Gamma_F^{(2)}[\phi]$  are the inverse two-point functions for the bosonic and fermionic fields, evaluated at the vacuum expectation value of the mesonic field  $\phi_0$ . Here, the boundary conditions of the functional integral appear in the momentum traces and we neglect contributions from mixed quark-meson-loops. In order to regularize the functional traces, we use the Schwinger proper time representation of the logarithms. We consider the effective action in a local potential approximation (LPA), which represents the lowest order in the derivative expansion and incorporates fermionic as well as bosonic contributions to the potential density  $U$ . In this approximation, the effective field  $\phi$  is considered to be constant over the entire volume.

The scale dependence is introduced through the infrared cut-off function  $f_a(k^2)$ , which regularizes the Schwinger proper time integral. A cut-off function of the form

$$k \frac{\partial}{\partial k} f_a(k^2) = -\frac{2}{(a+1)} (k^2)^{a+1} e^{-k^2} \quad (5)$$

satisfies the required regularization conditions [22, 23, 24, 31]. We obtain a renormalization group flow equation for the effective potential by performing a renormalization group improvement and replacing the bare two-point functions by the renormalized, scale-dependent two-point functions,

$$\begin{aligned} k \frac{\partial}{\partial k} Z_k[\phi] &= \frac{1}{2} \text{Tr}_{Z_0} \frac{d}{d k} k \frac{\partial}{\partial k} f_a(k^2) \exp[-Z_{B,k}^{(2)}[\phi]] \\ &\quad \text{Tr}_0 \frac{d}{d k} k \frac{\partial}{\partial k} f_a(k^2) \exp[-Z_{F,k}^{(2)}[\phi]] \end{aligned} \quad (6)$$

In LPA, the effective action reduces to the effective potential by the relation

$$Z_k[\phi] = d^4x U_k(\phi) \quad (7)$$

The renormalization group improved evolution equation for the effective potential in finite volume is given by

$$\begin{aligned} k \frac{\partial}{\partial k} U_k(\phi; L) &= \frac{1}{2} \int_0^Z \frac{d}{d k} \frac{d^4 p}{(2\pi)^4} n \exp[-(\vec{p}^2 + M_q^2(\phi; L))] \\ &\quad \exp[-(\vec{p}^2 + M^2(\phi; L))] - 3 \exp[-(\vec{p}^2 + M^2(\phi; L))] k \frac{\partial}{\partial k} f_a(k^2): \end{aligned} \quad (8)$$

It is necessary to choose the parameter  $a$  in such a way that the resulting integrals over the proper time parameter remain finite. In finite volume, the lowest possible integer value is  $a = 2$ . The diagonalization of the meson mass matrix gives the running meson masses which depend on the effective potential. Without explicit symmetry breaking, they are of the form

$$M^2 = 2 \frac{\partial^2 U_k}{\partial \phi^2} + 4 \frac{\partial^2 \partial^2 U_k}{\partial \phi^2 \partial^2} \quad (9)$$

$$M^2 = 2 \frac{\partial U_k}{\partial \phi^2} : \quad (10)$$

To derive renormalization group flow equations in the finite volume  $L^{d-1}$  at finite temperature  $T$ , we replace the integrals over the momenta by a sum

$$\sum_{n=1}^L \frac{2}{L} \frac{x^4}{n^2} : \quad (11)$$

and apply periodic boundary conditions for bosons and anti-periodic boundary conditions for fermions in time and space-like directions. The sums run from  $-1$  to  $+1$ , where the vector  $\mathbf{n}$  denotes  $(n_1; n_2; \dots; n_{d-1})$ . The Matsubara frequencies take the value  $\omega_n = 2\pi n T$  for bosons and  $\omega_n = (2n+1)\pi T$  for fermions, respectively. In the following we use the short-hand notation

$$p_F^2 = \sum_{i=1}^{X-1} p_i^2 = \frac{4\pi^2}{L^2} \sum_{i=1}^{X-1} n_i + \frac{1}{2}^2 \quad (12)$$

$$p_B^2 = \sum_{i=1}^{X-1} p_i^2 = \frac{4\pi^2}{L^2} \sum_{i=1}^{X-1} n_i^2; \quad (13)$$

for the momenta of the fermions and bosons, respectively. In finite volume, we allow explicit symmetry breaking in the effective potential, which then becomes a function of two variables and  $\omega^2$  separately. The corresponding expression to eq. (8) is

$$k \frac{\partial}{\partial k} U_k(\omega^2; L; T) = \frac{1}{2} \frac{T}{L^{d-1}} \sum_{i=1}^{X-1} \sum_{n=1}^N 4N_c N_f \exp(-\omega_i^2 + p_F^2 + M_i^2(\omega^2)) \exp(-\omega_i^2 + p_B^2 + M_i^2(\omega^2)) \sum_{a=1}^O k \frac{\partial}{\partial k} f_a(k^2); \quad (14)$$

The  $M_i^2$ ,  $i = 1, \dots, N_f^2$  are the eigenvalues of the second derivative matrix

$$U_k(\omega^2)^{ij} = \frac{\partial^2 U_k}{\partial \omega_i \partial \omega_j} \quad (15)$$

of the meson potential  $U_k(\omega^2)$  with respect to the fields  $\omega = (\omega_1, \dots, \omega_X)$ . They depend only on the magnitude of the pion fields  $\omega^2$  and are independent of the direction. We wish to stress the importance of this point, since otherwise the meson contributions from the low equations are not compatible with the ansatz for the potential which we will introduce below.

The second derivative matrix is given by

$$\begin{matrix} 0 & & & & 1 \\ & U & U_{\sim 2} & U_{\sim 2} & U_{\sim 2} & \\ \begin{matrix} B \\ B \\ B \\ B \\ B \\ B \\ @ \\ B \\ B \end{matrix} & U_{\sim 2} \\ & (1) & (1) & (1) & (1) & (1) \\ & 2U_{\sim 2} + U_{\sim 2\sim 2} 4 & (1)^2 & U_{\sim 2\sim 2} 4 & (1) & U_{\sim 2\sim 2} 4 \\ & & & (1) & (2) & (1) & (3) \\ & U_{\sim 2} \\ & (2) & (2) & (2) & (2) & (2) \\ & 2U_{\sim 2} + U_{\sim 2\sim 2} 4 & (2)^2 & 2U_{\sim 2} + U_{\sim 2\sim 2} 4 & (2) & 2U_{\sim 2} + U_{\sim 2\sim 2} 4 \\ & & & (2) & (3) & (2) & (3) \\ & U_{\sim 2} \\ & (3) & (3) & (3) & (3) & (3) \\ & U_{\sim 2\sim 2} 4 \\ & (1) & (2) & (3) & (2) & (3) \\ & & & (3) & (2) & (3) \\ & & & 2U_{\sim 2} + U_{\sim 2\sim 2} 4 & (3)^2 & \\ & & & & & \end{matrix} \quad (16)$$

where we have suppressed the scale index  $k$  of the potential and use the abbreviations

$$U = \frac{\partial U}{\partial \omega^2}; \quad U_{\sim 2}^{(a)} = \frac{\partial U}{\partial \omega^2} \frac{\partial \omega^2}{\partial (a)} = U_{\sim 2}^{(a)}; \quad U_{\sim 2} = \frac{\partial U}{\partial \omega^2}; \quad (17)$$

and the corresponding expressions for the higher derivatives. The eigenvalues of this matrix are given by

$$\begin{aligned} M_1^2 &= \frac{1}{2} 2U_{\sim 2} + 4\sim^2 U_{\sim 2\sim 2} + U + \frac{q}{(2U_{\sim 2} + 4\sim^2 U_{\sim 2\sim 2} - U)^2 + 16\sim^2 U_{\sim 2}^2}; \\ M_2^2 &= 2U_{\sim 2}; \quad M_3^2 = 2U_{\sim 2}; \\ M_4^2 &= \frac{1}{2} 2U_{\sim 2} + 4\sim^2 U_{\sim 2\sim 2} + U + \frac{q}{(2U_{\sim 2} + 4\sim^2 U_{\sim 2\sim 2} - U)^2 + 16\sim^2 U_{\sim 2}^2}; \end{aligned} \quad (18)$$

For vanishing cross terms  $U_{\sim 2}$ , the last eigenvalue reduces to  $2U_{\sim 2} + 4\sim^2 U_{\sim 2\sim 2}$ , which corresponds to a derivative in "radial" direction in the pion-subspace. Especially for  $\sim^2 = 0$ , the three pion modes have equal masses. We also note that the pion fields appear only in the combination  $\sim^2$  in the eigenvalues, despite the fact that the derivative matrix contains terms linear in  $\sim^2$ . The reason is that the rotational symmetry of the pion space remains unbroken even in the presence of explicit symmetry breaking terms in the sigma direction.

As discussed in [32], we are able to perform the sum over the thermal Matsubara frequencies analytically and obtain an evolution equation which contains the Fermi-Dirac distribution  $n_F(E)$  and the Bose-Einstein-distribution  $n_B(E)$ ,

$$k \frac{\partial}{\partial k} U_k(\sim^2; L; T) = \frac{(-1)^a}{2(a+1)} \frac{k^{2(a+1)}}{L^{d-1}} \frac{\partial^a}{(\partial k^2)^a} \sum_n \sum_{i=1}^4 \frac{X}{E_i} \frac{1}{(1 + 2n_B(E_i))} \frac{4N_c N_f}{E_q} (1 - 2n_F(E_q)); \quad (19)$$

with

$$n_F(E) = \frac{1}{e^{\frac{E}{T}} + 1}; \quad n_B(E) = \frac{1}{e^{\frac{E}{T}} - 1}; \quad (20)$$

where in the absence of a chemical potential for the fermions the Fermi-Dirac distributions for quarks and antiquarks coincide. The effective energies are defined by

$$E_q^2 = k^2 + p_F^2 + M_q^2(\sim^2); \quad E_i^2 = k^2 + p_B^2 + M_i^2(\sim^2); \quad (21)$$

The parameter  $a$  in the cutoff function is given by  $a = 2$  in the finite volume, in order to ensure that we can compare with the results in infinite volume. In the limit of vanishing temperature  $T = 0$ , we find in  $d = 4$  the finite volume evolution equation of the meson potential:

$$k \frac{\partial}{\partial k} U_k(\sim^2; L) = \frac{3}{16} \frac{k^6 X}{L^3} - \frac{4N_c N_f}{(E_q(\sim^2; L))^5} + \sum_{i=1}^4 \frac{X^4}{(E_i(\sim^2; L))^5} \quad (22)$$

The polynomial ansatz for the meson potential is determined by the following idea: Since the current quark mass is the only source of symmetry breaking, the quark term in the low equation determines the symmetry breaking terms of the potential. The constituent quark mass can be expanded around a finite expectation value of the mesonic fields, which is chosen in the direction of the field ,

$$\begin{aligned} M_q^2 &= g^2 [(\bar{q} + m_c)^2 + \bar{\pi}^2] = g^2 [(\bar{q}_0 + m_c)^2 + \bar{\pi}_0^2] \\ &= g^2 [(\bar{q}_0 + m_c)^2 + 2m_c(\bar{q}_0) + (\bar{q}_0^2 + \bar{\pi}_0^2)]: \end{aligned} \quad (23)$$

We have rescaled  $m_c$  by a factor  $g$  for convenience, so that the physical current quark mass is given by  $gm_c$ . From this expression, we read off that the contributions to the potential from the fermionic terms in the low equations can all be expressed in terms of powers of the combinations  $(\bar{q}_0^2 + \bar{\pi}_0^2)$  for the symmetric part and  $(\bar{q}_0)$  for the symmetry breaking parts. Therefore, we make for the meson potential the ansatz

$$U_k(\bar{q}; \bar{\pi}^2) = \sum_{i=0}^{\infty} \sum_{j=0}^{\infty} a_{ij}(k) (\bar{q}_0)^i (\bar{q}_0^2 + \bar{\pi}_0^2)^j \quad (24)$$

The low equations for the coefficients in this potential are derived in the appendix.

Incorporating the explicit breaking of the chiral symmetry into the potential and the low from the start has several advantages. The polynomial expansion above evolves automatically from a potential with small symmetry breaking peaked around  $h_i = 0$  to a potential with large symmetry breaking peaked at a value  $h_i = f$ . Without explicit symmetry breaking, the polynomial expansion in  $\bar{q}^2$  has to be changed from a parametrization in terms of powers of  $\bar{q}^2$  to  $(\bar{q}_0^2 + \bar{\pi}_0^2)$  at the chiral symmetry breaking scale [22].

As is well known, a linear symmetry breaking term remains unchanged in the renormalization group low [33]. Therefore the usual strategy is to evolve the potential without a symmetry breaking term. Explicit symmetry breaking is then taken into account after the quantum fluctuations have been integrated out on all scales [22, 29, 30]. In an infinite volume and for small quark masses, this is perfectly acceptable and will yield the correct results. In a finite volume, however, the situation is different. Since chiral symmetry is not spontaneously broken, explicit symmetry breaking has to be included on all scales in the renormalization group low to obtain a nonzero value for the order parameter. Otherwise, divergences from massless Goldstone bosons would restore the symmetry. In this context,

we would like to point out that even in the absence of a symmetry breaking term, the pion decay constant does not remain zero on all renormalization scales  $k$ . On some intermediate scale below the chiral symmetry breaking scale,  $k < k_c$ , where the quantum fluctuations are only partially integrated out, it acquires a nonzero expectation value, and chiral symmetry is spontaneously broken. However, the emergence of exactly massless Goldstone bosons dominates the infrared evolution of the potential and counteracts the formation of a symmetry breaking condensate.

When the potential is expanded in a polynomial in a theory with exactly massless Goldstone bosons, divergences appear in the flow equations for the coefficients of operators of mass dimension higher than four [24]. As an added benefit of including explicit symmetry breaking, the presence of a finite pion mass regulates these IR divergences.

#### IV. NUMERICAL EVALUATION

We have solved the RG flow equations numerically and present the results for the volume dependence of the pion mass and the pion decay constant in the following section. First we discuss our choice of model parameters at the UV scale, and some details of the numerical evaluation.

At the ultraviolet scale  $\mu_{UV}$ , the free parameters of the quark-meson model are the meson mass  $m_{UV}$ , the four-meson-coupling  $\mu_{UV}$ , and the current quark mass  $g m_c$ , which controls the degree of explicit symmetry breaking. The Yukawa coupling  $g$  does not evolve in the present approximation [22, 29, 30]. We choose  $g = 3.26$ , which leads to a reasonable constituent quark mass of  $M_q = g(f + m_c) = 310 \text{ MeV}$  for physical values for the pion decay constant  $f = 93 \text{ MeV}$  and the current quark mass  $g m_c = 7 \text{ MeV}$ .

In table I, we summarize the three parameter sets which we used in obtaining our results for pion masses of 100, 200 and 300 MeV. We determine these UV parameters by fitting to a particular value for the pion mass  $m(L)$  and to the corresponding value for the pion decay constant  $f(L)$  in finite volume. We then evolve the RG equations with these parameters to predict the volume dependence of  $f(L)$  and  $m(L)$ .

For any value of the pion mass, the corresponding value of the pion decay constant is taken from chiral perturbation theory [9]. The pion mass is mainly controlled by the value of the current quark mass, which parametrizes the symmetry breaking. The current quark

$_{\text{UV}}$ M eV	$m_{\text{UV}}$ M eV	$_{\text{UV}}$ M eV	$g m_c$ M eV	$f$ M eV	$m$ M eV
1500	779.0	60	2.10	90.38	100.8
1500	747.7	60	9.85	96.91	200.1
1500	698.0	60	25.70	105.30	300.2

TABLE I: Values for the parameters at the UV-scale used in the numerical evaluation. The parameters are determined in infinite volume by fitting to a particular pion mass and the corresponding value of the pion decay constant, taken from chiral perturbation theory. Note that in our notation, the physical current quark mass corresponds to  $g m_c$ .

mass varies from approximately 2 M eV for a pion mass of 100 M eV to about 10 M eV for  $m = 200$  M eV, it has to be increased to approximately 25 M eV for  $m = 300$  M eV. To achieve the correct corresponding values for the pion decay constant, the meson mass at the UV scale has to be decreased from approximately  $m_{\text{UV}} = 780$  M eV to  $m_{\text{UV}} = 700$  M eV, while the pion mass increases from 100 to 300 M eV. The four-meson-coupling  $_{\text{UV}}$  is fixed. We have checked that our results are to a very large degree independent of the particular choice of UV parameters: Different sets of parameters leading to the same values of the low-energy constants in the infinite volume give the same volume dependence.

Although it facilitates the comparison to chiral perturbation theory, it is not necessary as a matter of principle to use the chiral perturbation theory result for the mass dependence of the pion decay constant. However, as has been found for infinite volume, in order to correctly describe the behavior of the pion decay constant as a function of a single symmetry breaking parameter, it is necessary to go beyond the approximation of a constant expectation value for the meson field, which we used in this paper, and to include wave function renormalizations in the RG flow [27]. This makes it possible to recover the correct prefactors of chiral logarithms in the framework of the renormalization group. Such an approach is more powerful than the present one, since in addition to the volume dependence, it predicts the dependence of  $m$  and  $f$  on the symmetry breaking parameter  $m_c$ . We stress that even in such an approach, it remains necessary to fit the parameters at the UV scale to the correct values of the low energy constants. Thus, for example the value of the pion decay constant in the chiral limit is not a prediction of the model, but a necessary input to constrain its parameters. The full set of RG-equations including the wave function renormalization and coupling constant

renormalization equations would reduce the input parameters to the four fermion coupling and the current quark mass at the UV-scale. In connection with the symmetry breaking ansatz eq. (24), these equations are more complicated and have not been worked out yet.

A limit on the possible values of the current quark mass is given by the requirement that all masses, in particular the sigma-mass, remain substantially smaller than the ultraviolet cutoff  $_{UV} = 1500 \text{ MeV}$  of the model. For a pion mass of  $m = 300 \text{ MeV}$ , we find  $m = 800 \text{ MeV}$ .

With regard to the UV-cutoff, we find only a slight dependence of our results for reasonably large volumes. When we change the cutoff from  $_{UV} = 1500 \text{ MeV}$  to  $_{UV} = 1100 \text{ MeV}$ , our results for the relative shift  $R[m(L)]$  of the pion mass in the finite volume change little. The change in the pion mass from a variation of the cutoff is of the order of less than 1% for  $L > 2 \text{ fm}$ , and approximately 6% at  $L = 1 \text{ fm}$  for the largest pion mass we considered here,  $m = 300 \text{ MeV}$ . For smaller pion mass, the dependence on the UV cutoff becomes weaker, for  $m = 100 \text{ MeV}$  it is negligible on the scale of our results. This can be understood, since a higher degree of explicit symmetry breaking leads to more massive particles for which a smaller value for the UV momentum cutoff becomes more relevant.

The sums over the momentum modes in the flow equations cannot be performed analytically. For a numerical evaluation of the flow equations, these sums must be truncated at a maximal mode number  $N_{max} = \max_j j$  which defines the cutoff momentum mode  $p_{max} = \frac{2}{L} N_{max}$ . This numerical truncation should not introduce an additional UV cutoff in the model, and therefore we require that

$$\frac{2}{L} N_{max} \ll_{UV} : \quad (25)$$

Since we use a "soft" cutoff function it is necessary to really satisfy the above equation with a safe margin. For the volumes with  $L = 1 \text{ fm}$  considered here, we have used  $N_{max} = 40$ .

In figure 1, the dependence of the relative difference of the pion mass in finite volume from its value in the infinite volume limit,  $R[m(L)]$ , is shown as a function of  $L$  for different values of the maximal mode number  $N_{max}$ . The relative mass difference depends mainly on  $m L$  and drops exponentially for large values of this dimensionless variable. Thus, for any given value of  $L$ , the value of  $R[m(L)]$  will be smaller for a heavier pion. Comparing the two panels in figure 1, we see that although the absolute values are smaller, the relative error due to the finite number of momentum modes in the evaluation is larger for a heavier

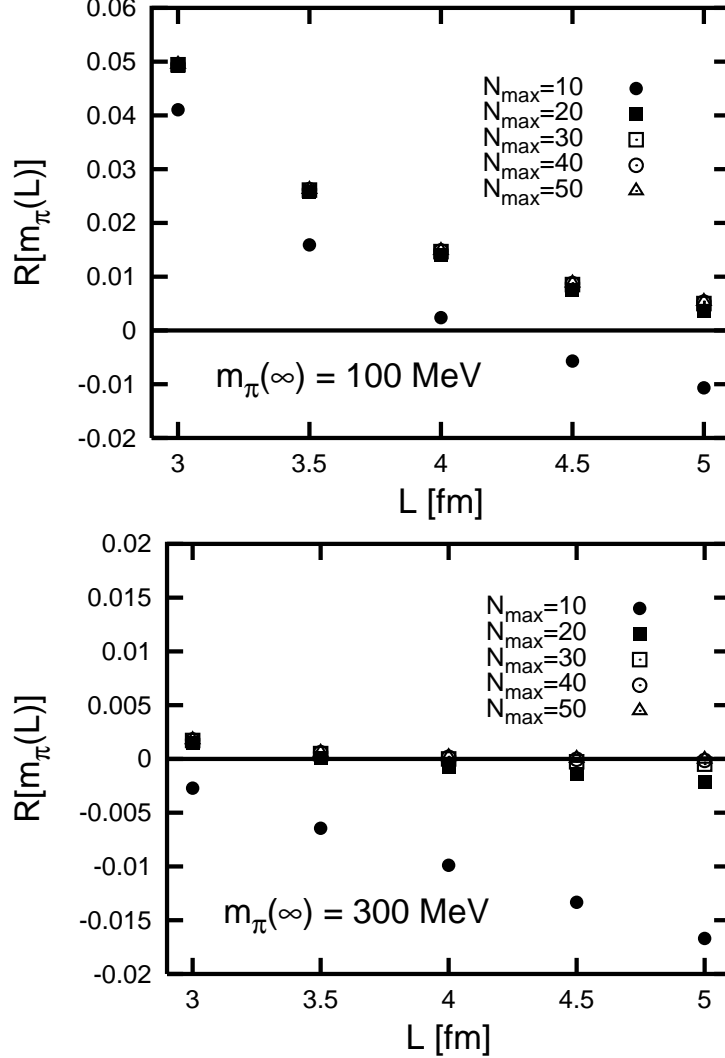


FIG. 1: The figures show the dependence of the results for the pion mass in finite volume on the truncation  $N_{\max}$  of the momentum sum in the numerical evaluation of the flow equations. Plotted is  $R[m_\pi(L)]$ , the relative deviation of the finite volume pion mass from the value in infinite volume, as a function of the box size  $L$ , for different values of  $N_{\max}$ . Results for two different values of the pion mass are shown in the two panels. Ideally, for large volumes, the relative deviation from the infinite volume pion mass should approach zero. The truncation has a relatively larger effect for heavier pion masses.

pion. The reason is the increasing importance of the non-zero momentum modes when the pion mass becomes larger at fixed box size. Following the argument from [11] outlined above, if  $1=m \ll L$ , then the partition function is dominated by the zero modes and effects from finite momentum modes present small corrections. When the pion mass is increased,

the importance of the finite momentum modes grows and the number of modes has to be increased to obtain results with the same level of accuracy. This argument can be presented in a more formal way. The momentum sums contributing to the flow equations are of the form

$$\frac{X}{n_1 n_2 n_3} \frac{1}{k^2 + m^2 + n^2 \frac{4}{L^2}} \quad (26)$$

where  $n^2 = n_1^2 + n_2^2 + n_3^2$ . For small values of the renormalization scale  $k$ , the sum is dominated by the zero mode term

$$\frac{1}{m^2} + \frac{1}{m^2 + \frac{4}{L^2}} + \dots \quad (27)$$

If the box is sufficiently small, all terms with non-zero momentum are suppressed by  $1=L^2$ , which acts as a large regulator. As we increase the size of the box, so that  $1=L \ll m$ , the contributions of the nonzero momentum modes are of the same size as the zero mode term. Therefore, effects from a truncation of the momentum sums should be expected to appear already at a smaller box size for large pion masses, which is exactly what we observe.

## V. RESULTS

The results of the RG-flow equations for the evolution with the infrared cutoff scale  $k$  give a picture of chiral symmetry breaking which reflects the formation of the quark condensate for higher momenta and the effects of pion fluctuations at low scales. Figure 2 shows the masses of the pion and sigma, and the pion decay constant as a function of the renormalization scale  $k$ , for a value of  $m = 100$  MeV, in the infinite volume limit. Starting at the UV scale  $k_{UV}$  and proceeding towards smaller values of  $k$ , we observe that the pion decay constant  $f$  grows rapidly around the chiral symmetry breaking scale  $k_{SB} \approx 800$  MeV, begins to flatten between 600–400 MeV, and becomes almost completely flat below 300 MeV. Generally, massive degrees of freedom decouple from the renormalization group flow at a momentum scale given by the value of their mass  $m$ , i.e. they do not contribute to the renormalization for  $k < m$ . This can be seen clearly in the flow of  $f$ . As soon as the renormalization scale is of the order of the constituent quark mass (approximately 300 MeV), the quarks are no longer dynamical degrees of freedom and  $f$  becomes essentially constant. The RG flow of the mass of the heaviest meson, the sigma, is in several respects

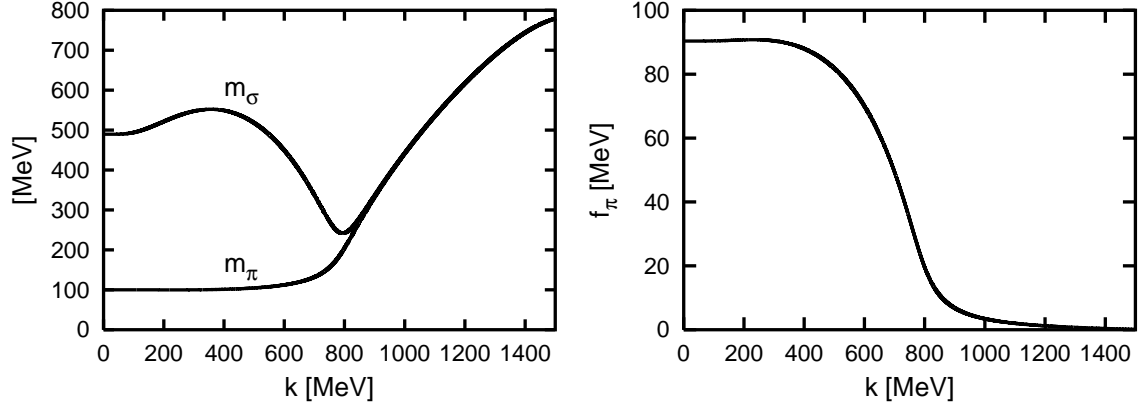


FIG. 2: Masses of the mesonic degrees of freedom and the pion decay constant as a function of the renormalization scale  $k$  in finite volume. The chiral symmetry breaking scale can be clearly identified as the scale at which the mass of heaviest meson (the  $\sigma$ ) has a minimum. For this figure, we have chosen  $m(1) = 100$  MeV and  $f(1) = 90.4$  MeV.

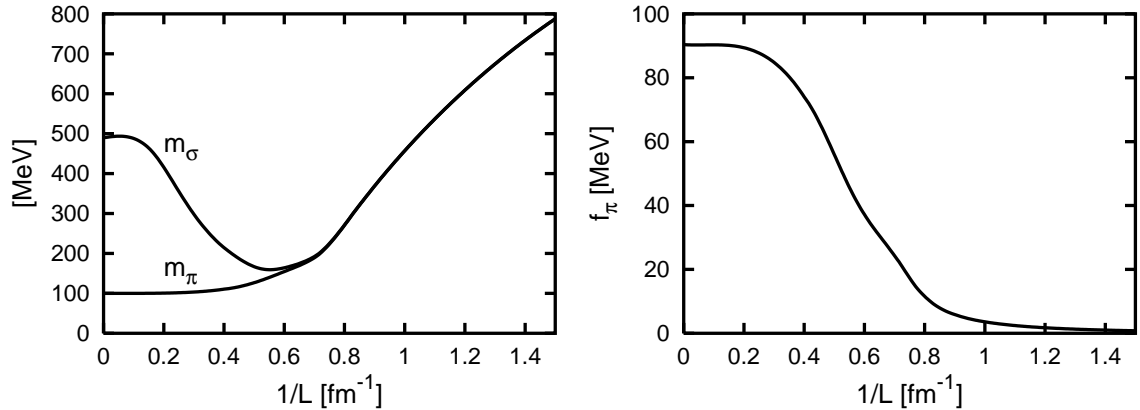


FIG. 3: Masses of the mesonic degrees of freedom and the pion decay constant as a function of the inverse box size  $1=L$ . The results are obtained by completely integrating out all quantum fluctuations ( $k \neq 0$ ) at fixed  $L$ . As soon as  $k < 1=L$ , the box size becomes the controlling scale, and in the limit  $k \rightarrow 0$  it is the only scale that remains. As for the preceding figures, we show the results with  $m = 100$  MeV and  $f = 90.4$  MeV for  $k \neq 0$  and  $L \neq 1$ .

very similar to the flow off. Its slope is also initially large at the chiral symmetry breaking scale and starts to decrease between 600 – 400 MeV as well. The value of the sigma mass reaches a maximum at  $k$  slightly above 300 MeV. Its decrease below this scale is due to the light pion with a mass of 100 MeV, which remains in the evolution as the only

dynamical degree of freedom. When the pion mass is increased, the drop in the sigma mass below the scale set by the constituent quark mass becomes much less pronounced. For  $m_q = 300 \text{ MeV}$ ,  $m(k)$  is essentially a flat function of  $k$  after it has reached its maximum.

In finite volume, a similar behavior is visible. In figure 3, the meson masses and the pion decay constant are shown as a function of the scale  $1=L$  set by the finite volume. In these results, all quantum fluctuations are integrated out completely, which removes the scale  $k$ . Now let us consider a finite value of  $k$ , where the quantum fluctuations are only partially integrated out. The scale  $1=L$  introduced by the finite volume is in competition with the renormalization scale  $k$ . As soon as  $k$  drops below  $=L$ , the renormalization scale no longer controls the renormalization flow. We can interpret the results shown in fig 3 roughly as an instant picture of the  $k$ -flow arrested at a scale  $k = =L$ . However, this correspondence is not one-to-one: while the cut-off affects both bosonic and fermionic fields in the same way, this is not true for  $1=L$ . Since there are no zero modes for fields with anti-periodic boundary conditions, the fermionic fields are more strongly affected by this cut-off than the mesons. For the mesons, the scale  $\frac{2}{L}$  imposes only a minimum value for the smallest non-zero momentum mode. For the fermionic fields, on the other hand, the lowest momentum mode  $\vec{p} = \vec{L}$  can effectively "freeze" the quark fields already above the constituent quark mass scale and no condensation of quarks takes place. For very small volumes  $1=L > 0.5 \text{ fm}^{-1}$ , the suppression of quark condensation by the large cut-off becomes the dominating effect. The chiral symmetry is approximately restored. A more subtle effect can also be seen in the behavior of the sigma-mass. While the sigma-mass has a maximum in the  $k$ -flow at a value of  $m = 600 \text{ MeV}$ , from which it drops to  $m = 500 \text{ MeV}$  due to the pion fluctuations, there is no corresponding maximum in the  $1=L$ -dependence. With decreasing  $1=L$  the pions hardly feel the constraints of the finite volume, but the momentum scale at which the quarks decouple consistently increases. Therefore the pion contributions at low momenta have a greater effect in the RG flow, since the  $k$ -region increases in which they are the only relevant degrees of freedom. Through this effect, the pions also contribute toward the restoration of chiral symmetry for small volumes.

The volume dependence of the low energy observables are the main results of this paper. In table II, we give the values for  $R[m(L)]$ , cf. eq. (1), the relative difference of the pion mass  $m(L)$  in finite volume from its value in infinite volume, for three volume sizes

			R [m (L)]							
L [fm]	m (1) [MeV]	m L	RG		1L chPT		+ (nnlo-lo)		R	
2.0	100	1.01293	26.6	$10^{-2}$	8.74	$10^{-2}$	11.6	$10^{-2}$	15.0	$10^{-2}$
	200	2.02586	5.38	$10^{-2}$	2.00	$10^{-2}$	3.31	$10^{-2}$	2.07	$10^{-2}$
	300	3.03879	1.70	$10^{-2}$	0.56	$10^{-2}$	1.12	$10^{-2}$	0.58	$10^{-2}$
2.5	100	1.26616	10.37	$10^{-2}$	3.85	$10^{-2}$	4.97	$10^{-2}$	5.40	$10^{-2}$
	200	2.53233	1.95	$10^{-2}$	0.73	$10^{-2}$	1.17	$10^{-2}$	0.78	$10^{-2}$
	300	3.79849	5.31	$10^{-3}$	1.65	$10^{-3}$	3.27	$10^{-3}$	2.04	$10^{-3}$
3.0	100	1.5194	4.94	$10^{-2}$	1.91	$10^{-2}$	2.41	$10^{-2}$	2.53	$10^{-3}$
	200	3.03879	7.85	$10^{-3}$	2.95	$10^{-3}$	4.65	$10^{-3}$	3.20	$10^{-3}$
	300	4.55819	1.76	$10^{-3}$	0.54	$10^{-3}$	1.05	$10^{-3}$	0.71	$10^{-3}$

TABLE II: Values for  $R [m (L)]$ , cf. eq. (1), the relative shift of the pion mass in finite volumes of  $L = 2.0; 2.5; 3.0$  fm, compared to the value in infinite volume, for pion masses of  $m (1) = 100; 200; 300$  MeV. We compare our RG calculation to the exact one-loop chPT results of [11] for a finite volume (1L chPT), and the exact one-loop calculation with corrections in three-loop order obtained with chPT using Luscher's formula [9] (1L chPT + (nnlo-lo)). In the last column, the difference  $R$  between the RG result and the three-loop corrected chPT result is given.

$L = 2.0; 2.5; 3.0$  fm and three pion masses  $m (1) = 100; 200; 300$  MeV.

In figures 4 and 5, we show the relative change of the pion mass  $m (L)$  and the pion decay constant  $f (L)$  as a function of the size  $L$  of the three-dimensional volume. We plot the results for the relative differences on a logarithmic scale for three different values of the pion mass  $m (1) = 100; 200; 300$  MeV.

Let us first discuss the plots for the pion mass in fig. 4. The relative change of the pion mass decreases with the volume size  $L$  and the pion mass  $m (1)$ . Fig. 4 also contains the results of chiral perturbation theory from the exact one-loop calculation in infinite volume [10] and also the 'best estimate' from [9]. As discussed in section II, the difference between the results of Luscher's formula for the mass shift which uses as input  $\pi$ -scattering in the one-loop and three-(nnlo) loop order is used as a correction to the exact one-loop mass shift from [10].

Our RG results have the same slope as chiral perturbation theory, but are consistently

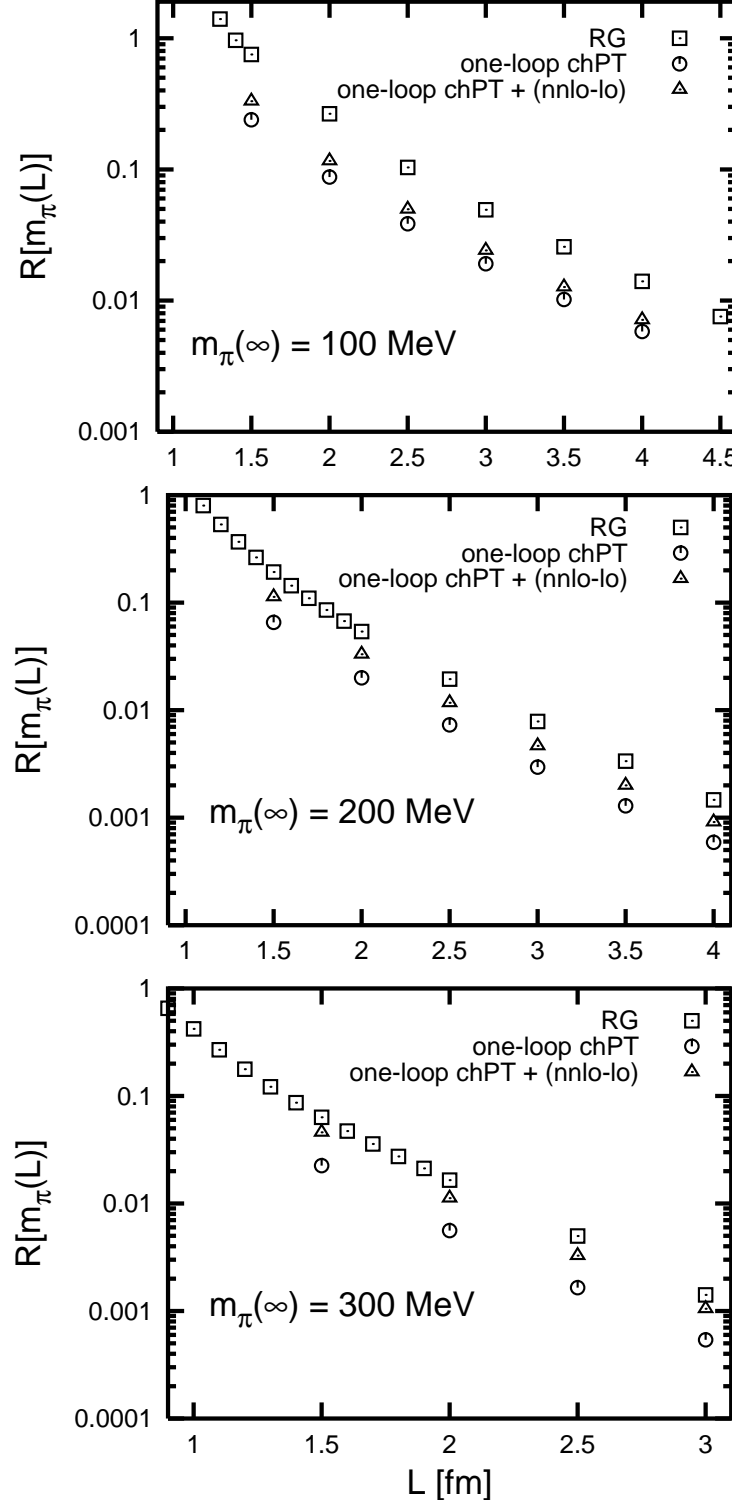


FIG . 4: Volume dependence of the pion mass. We plot the relative shift of the pion mass from its infinite volume limit  $R[m_\pi(L)] = (m_\pi(L) - m_\pi(1))/m_\pi(1)$  as a function of the size of the volume  $L$ . For comparison, we also plot the results from chPT calculations taken from [9]. The values for the pion mass in infinite volume are given in the figure, note the different scales on the axes for different  $m_\pi(1)$ .

above chiral perturbation theory, even with corrections to three loops. In general, the RG calculation gives values for  $R[f(L)]$  which are about a factor 1.5 to 2.0 larger than the values from chPT, as can be seen in table II.

The difference between the RG result and the loop expansion decreases with higher order in loops. The RG result is closer to the calculation with nnnL-Luscher formula than to the one loop chPT calculation.

For large volumes, the pion mass should drop as  $\exp(-m/L)$ . Therefore, we expect that the slope of the RG result is the same as that from chiral perturbation theory, which is indeed the case. The calculation with the flow equation can be continued to smaller box sizes, as long as the momenta constrained by the box are below the cut-off  $\mu_V$ . The slope of the RG result at small box size ( $L < 1 \text{ fm}$ ) is approximately given by the meson mass  $m = m_\pi$ , cf. fig. 3, after the transition between the regime dominated by chiral symmetry breaking and the one with restored chiral symmetry has taken place. In this other region the chiral expansion can no longer be considered reliable and is therefore no longer applied.

While the relative difference between the exact one-loop result and the RG results remains approximately constant for different pion masses, the relative difference between the RG results and the results of Colangelo and Durr [9] decreases when the mass of the pion is increased. We have checked that the difference between our RG results and the chiral perturbation theory results from Colangelo and Durr are consistent with the error estimate of Luscher's approximation formula. We find for all pion masses that the differences decrease exponentially according to  $\exp(-Cm/L)$ , with  $C$  a positive constant of order 1.

Next we discuss the results for the volume dependence of the pion decay constant shown in fig. 5. As for the pion mass, we compare with the chiral perturbation theory results [10] and [8]. Note that in this case, we define the relative difference with opposite sign as  $R[f(L)] = (f(1) - f(L))/f(1)$ , because the pion decay constant is smaller for a finite volume, in contrast to the pion mass. We refer to fig. 3 for an illustration of the global behavior of  $f(L)$ . When the size of the volume is decreased, the pion decay constant at first drops only slowly, and then sharply at the scale associated with chiral symmetry breaking. For very small volumes, the pion decay constant vanishes and chiral symmetry is effectively restored. This is true for  $L \rightarrow 0$  regardless of the value of the pion mass. Therefore, the largest possible relative shift for  $L \rightarrow 0$  is  $R[f(0)] = 1$ , when the order parameter vanishes completely.

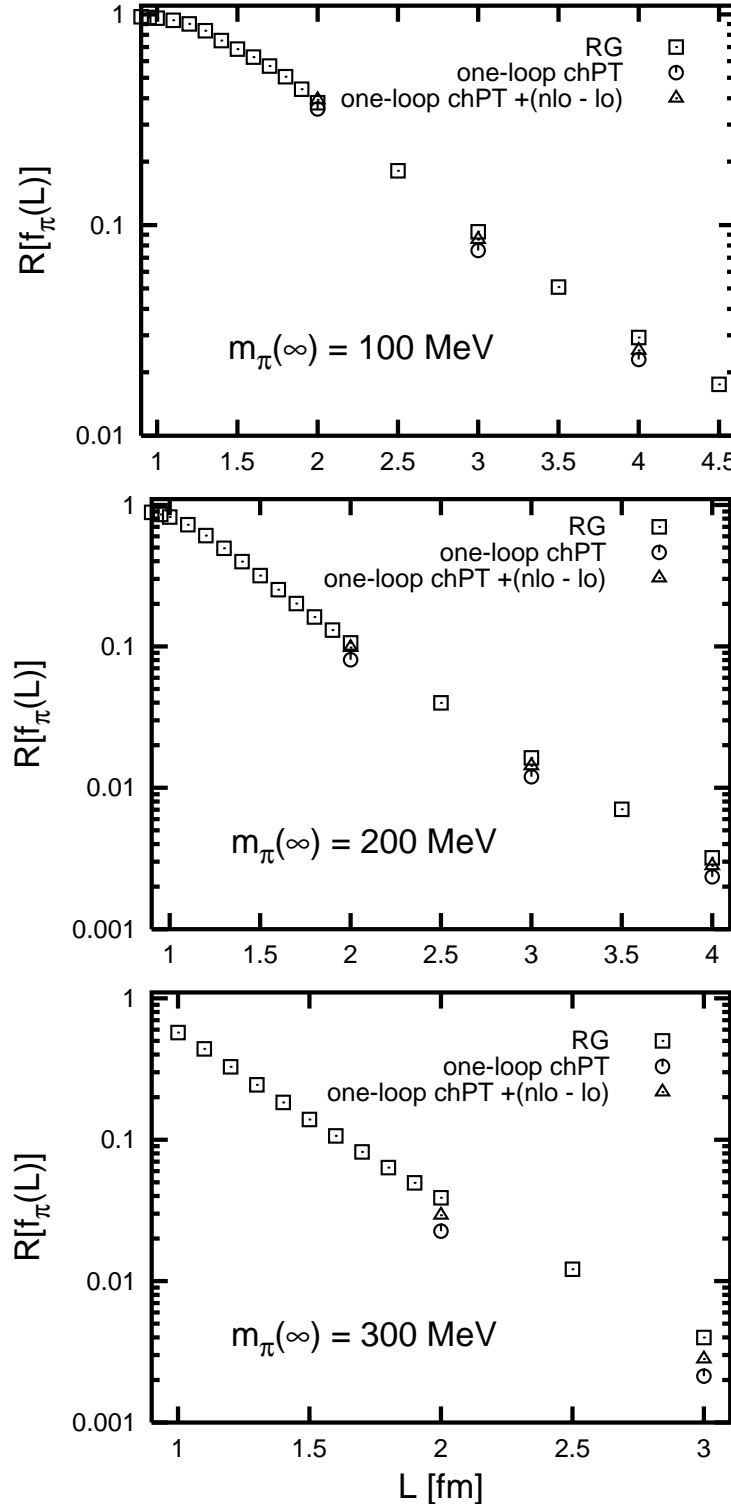


FIG. 5: Volume dependence of the pion decay constant. We plot the relative shift from the infinite volume limit  $R_f(L) = (f(1) - f(L))/f(1)$  as a function of the box size  $L$  for different values of the pion mass. For comparison, we show the chPT results taken from [8]. The values from (1) are given in the panels. Note the different scales on the axes for different  $m_\pi(\infty)$ .

The plots for the volume dependence of  $f$  illustrate in which region chiral perturbation theory remains valid. Since spontaneously broken chiral symmetry and a sufficiently large  $f$  are required, chPT does not describe the transition to the region with effectively restored chiral symmetry. Therefore, chiral perturbation theory results are available only for volumes with  $L = 2 \text{ fm}$ . Already for  $L = 2 \text{ fm}$  and a pion mass  $m = 100 \text{ MeV}$ , the  $f$ -shift is almost 40%. The RG method remains valid in both regions, down to very small volumes.

We compare with the chiral perturbation theory results obtained by using an approximation similar to Lüscher's formula for the pion mass shift, which was derived in [8]. For the pion decay constant, the input needed to calculate the finite volume shift is an amplitude involving the axial current in finite volume. So far only two loops in chiral perturbation theory (nb) are known. The chPT nb-corrections to the exact one-loop result increase the shift towards larger values. As in the case of the pion mass, the RG results give a slightly larger finite volume shift than the chPT results. Again the results from RG and chPT converge for larger values of the pion mass (note the different scales on both axes in the plots for different values of  $m$ !).

For the volume dependence of the sigma-mass, we refer back to fig. 3, where we show the overall dependence of  $m$  on  $1=L$ . It is interesting to relate the variation of  $m$  ( $1=L$ ) to the  $0^{++}$  phase shift of  $\pi$ -scattering, which will be done in a separate work.

## V I. CONCLUSIONS

We have presented a new approach to the quark-meson-model employing the renormalization group method in a finite volume within the framework of the Schwinger proper time formalism. Central to any such approach is the inclusion of explicit chiral symmetry breaking. Since chiral symmetry is not broken spontaneously in a finite volume, it is necessary to introduce a finite current quark mass. In this paper, we have evolved the effective potential with additional symmetry-breaking terms. The form of these terms is constrained by the quark contributions to the renormalization group flow, which introduce the explicit chiral symmetry breaking.

By solving the resulting renormalization group flow equations numerically, we have obtained results for the volume dependence of the meson masses, in particular the pion mass, and the pion decay constant, the order parameter of chiral symmetry breaking.

Our results show consistently a larger finite volume mass shift for the pion than has been obtained in chiral perturbation theory including up to three loops. The differences between the chiral perturbation theory results which make use of the Luscher formula and the RG results obtained in the present paper are consistent with the error estimate for Luscher's approximation. As one expects, the difference is largest for small values of  $m/L$ . We have checked that this difference decreases exponentially with an increase in this dimensionless quantity. As shown in figs. 4, 5, our results and those obtained in chiral perturbation theory with Luscher's formula [8, 9] converge for large current quark masses. We note that the ratio of the results from chPT and RG does not depend on  $L$ , even down to  $L = 1.5$  fm.

Compared to the present numerical approach, chiral perturbation theory has the advantage that it is possible to obtain analytic expressions for the finite volume mass shift. This makes comparisons to lattice results simpler. On the other hand, current lattice volumes and lattice pion masses are at the edge of a reliable chiral perturbation theory calculation. In contrast, the RG method remains valid for large current quark masses as well as small volumes.

The main uncertainty of the RG method comes from its dependence on the UV cut-off scale  $\mu_V$  for large meson masses. The system becomes sensitive to  $\mu_V$  for large explicit symmetry breaking, because the mass of the sigma as the heaviest particle approaches the UV cut-off. For a pion mass of  $m = 300$  MeV, the sigma mass is  $m = 800$  MeV. In this case, a cut-off variation between  $\mu_V = 1500$  MeV and 1100 MeV, changes the pion mass for a volume with  $L = 1$  fm by approximately 6%, and by less than 1% for  $L > 2$  fm. Within this uncertainty, our results agree with those of chPT for  $m = 300$  MeV. In contrast, for  $m = 100$  MeV the cut-off dependence is so weak that it is not noticeable on the scale of the results. The RG and chPT results do not agree within this uncertainty, cf. table II for  $m = 100$  MeV and  $m = 200$  MeV.

The dependence of our results on the choice of model parameters at the UV scale is much weaker than that on the cut-off. By fitting to the values of the low-energy observables  $m$  and  $f$  in finite volume, we achieve a very high degree of independence on the particular choice of UV parameters.

We expect that the inclusion of wave function renormalizations in the finite volume renormalization group flow should make it possible to describe the low energy constants as a function of a single symmetry breaking parameter, the quark mass  $m_c$ . It has already

been observed that this is the case in infinite volume, where the behavior of  $m$  and  $f$  as a function of  $m_c$  is described correctly when all other UV parameters remain fixed [27]. Systematic errors introduced by the simplification used in this paper to adjust both  $m$  (1) and  $f$  (1) in infinite volume could then be estimated by a comparison of the calculations.

Although we have not yet investigated these questions in depth, it appears that the present approach, which treats the pion fields and the sigma explicitly and as individual degrees of freedom, proves the convergence [24] of the polynomial expansion of the effective potential. This is due to the finite mass acquired by the Goldstone bosons, which becomes relevant for  $k \neq 0$ .

The RG approach shows in a transparent way the relevance of the momentum scale introduced by the finite volume for the quantum fluctuations.

#### Acknowledgments

H.J.P. would like to thank Prof. Leutwyler and Dr. Durr for instructive discussions. J.B. would like thank the GSI for financial support.

#### APPENDIX A : FLOW EQUATIONS

We derive now equations for the coefficients of the potential by inserting eq. (24) into the flow equation for the potential and comparing coefficients of both sides. We define expansion coefficients for the flow equations:

$$k \frac{\partial}{\partial k} U_k^{ij} = \frac{1}{i! j!} \frac{\partial}{\partial}^i \frac{\partial}{\partial^2}^j k \frac{\partial}{\partial k} U_k = 0 : \quad (A1)$$

Then the flow equations for the coefficients  $a_{ij}$  in the ansatz for the potential are given by

$$\begin{aligned} k \frac{\partial}{\partial k} U_k^{ij} &= k \frac{\partial}{\partial k} a_{ij} + a_{i+1,j} - k \frac{\partial}{\partial k}^0 (i+1)(1-N_{ij}) \\ &\quad + a_{i,j+1} (j+1) - 2 a_{0k} \frac{\partial}{\partial k}^0 (1 - \frac{1}{2} N_{ij}) \end{aligned} \quad (A2)$$

with the additional condition that  $(1+2j) \leq N$ .

In order for  $a = 0$  to actually correspond to a minimum of the potential, it must satisfy  $\frac{\partial}{\partial} U_k|_{j=0} = 0$ . For the coefficients  $a_{10}$  and  $a_{01}$ , this translates into the condition

$$a_{10} + 2a_{01} = 0 : \quad (A3)$$

Due to this condition, only two of the variables in the set  $a_{10}, a_{01}, \phi$  are independent, and the third one can be expressed in terms of the other two. Likewise, if we take the derivative of the equation (A 3) with respect to the renormalization scale  $k$ , we get an equation which relates the flow of these three variables:

$$k \frac{\partial}{\partial k} a_{10} + 2a_{01}k \frac{\partial}{\partial k} \phi + 2 \phi k \frac{\partial}{\partial k} a_{01} = 0: \quad (\text{A 4})$$

We can use this equation to replace the flow equation for  $a_{10}$  in the above set eq. (A 2). It is desirable to eliminate  $a_{10}$ , since  $\phi$  and  $a_{01}$  both correspond to the observables we wish to obtain, namely the pion decay constant and the pion mass. In addition, with this replacement the system of differential equations can also be solved more easily.

From the general expression for the flow equations eq. (A 2), we find the particular equations governing  $a_{10}$  and  $a_{01}$ :

$$k \frac{\partial}{\partial k} U_k^{10} = k \frac{\partial}{\partial k} a_{10} - 2a_{01}k \frac{\partial}{\partial k} \phi - a_{11} - 2 \phi k \frac{\partial}{\partial k} \phi \quad (\text{A 5})$$

$$k \frac{\partial}{\partial k} U_k^{01} = k \frac{\partial}{\partial k} a_{01} - a_{11}k \frac{\partial}{\partial k} \phi - 2a_{02} - 2 \phi k \frac{\partial}{\partial k} \phi : \quad (\text{A 6})$$

The flow equation for  $a_{10}$  contains on the LHS only terms that are proportional to the symmetry-breaking current quark mass  $m_c$ . Because of this,  $a_{10}$  does not evolve in the chiral limit  $m_c \rightarrow 0$ . If it is initially zero at the UV scale, it remains zero on all scales. In this case, the condition (A 4) forces the coefficient  $a_{01}$  to vanish as soon as  $\phi$  acquires a finite expectation value. This corresponds to the appearance of exactly massless Goldstone bosons in case of spontaneous symmetry breaking, in accordance with our expectations for the chiral limit.

In order to derive a flow equation for the minimum of the potential  $\phi$ , we can combine the two equations and use eq. (A 4) to eliminate the  $k$ -derivatives of  $a_{10}$  and  $a_{01}$ :

$$k \frac{\partial}{\partial k} U_k^{10} + 2 \phi k \frac{\partial}{\partial k} U_k^{01} = k \frac{\partial}{\partial k} \phi (2a_{20} + 2a_{01} + 4a_{11} \phi + 8a_{02} \phi^2) : \quad (\text{A 7})$$

From the expressions for the meson masses, evaluated at the minimum of the potential, it can be seen that the expression in brackets, which multiplies the  $k$ -derivative of  $\phi$ , is up to a constant factor the square of the mass,  $M^2$ . Therefore, this equation is always well-conditioned. The only exception is at the chiral symmetry breaking scale, where  $M^2$  drops sharply, if the explicit symmetry breaking is very small. For reasonably large pion masses, this is not a problem.

## APPENDIX B : ANSATZ FOR THE POTENTIAL

We use the flow equations in infinite volume to motivate the ansatz for the potential with explicit symmetry breaking. Neglecting the mesonic contributions to the flow equations, we are left with the terms arising from the fermions:

$$k \frac{\partial}{\partial k} U^F ( ; \sim^2) = \frac{4N_f N_c}{32^2} \frac{k^6}{k^2 + M_q^2} : \quad (B1)$$

The constituent quark mass  $M_q$  contains through the current quark mass  $m_c$  the only explicitly symmetry breaking term in the flow equation. As shown in eq. (23), by expanding around the minimum of the potential, the quark mass can be written as

$$M_q^2 = g^2 [( \bar{0} + m_c)^2 + 2m_c ( \bar{0} + ( \bar{2} + \sim^2 \bar{0}^2))] ; \quad (B2)$$

where  $m_c$  is rescaled by a factor of  $g$  for convenience. When we expand the denominator in the flow equation in the deviation of the fields from the vacuum expectation value, the result contains only those terms we postulated in our ansatz for the potential:

$$\begin{aligned} k \frac{\partial}{\partial k} U^F ( ; \sim^2) = & \frac{1}{32^2} 4N_f N_c \frac{k^6}{k^2 + g^2 ( \bar{0} + m_c)^2} \\ & ( \bar{2} + \sim^2 \bar{0}^2) \quad " \quad \frac{g^2}{k^2 + g^2 ( \bar{0} + m_c)^2} \quad \# \\ & + ( \bar{2} + \sim^2 \bar{0}^2)^2 \quad " \quad \frac{g^2}{k^2 + g^2 ( \bar{0} + m_c)^2} \quad \# \\ & + ( \bar{0} + 2m_c) \quad " \quad \frac{g^2}{k^2 + g^2 ( \bar{0} + m_c)^2} \quad \# \\ & + ( \bar{0})^2 \quad 4m_c^2 \quad " \quad \frac{g^2}{k^2 + g^2 ( \bar{0} + m_c)^2} \quad \# \\ & + ( \bar{0}) ( \bar{2} + \sim^2 \bar{0}^2) 2 \quad 2m_c \quad " \quad \frac{g^2}{k^2 + g^2 ( \bar{0} + m_c)^2} \quad \# \\ & ) \\ & + \dots : \end{aligned} \quad (B3)$$

All remaining terms are of higher order in  $( \bar{0})$  or  $( \bar{2} + \sim^2 \bar{0}^2)$  or any combination thereof. Only the terms in  $( \bar{2} + \sim^2 \bar{0}^2) = ( \bar{2} \bar{0}^2)$  remain in the chiral limit  $m_c \rightarrow 0$ .

These terms respect the chiral symmetry and the potential reduces to the symmetric form .

---

- [1] D .Becirevic and G .V illadoro, Phys. Rev. D 69 (2004) 054010 [arX iv:hep-lat/0311028].
- [2] A .A liK han et al [QCD SF-UK QCD Collaboration], Nucl. Phys. B 689 (2004) 175 [arX iv:hep-lat/0312030].
- [3] M .G uagnelli, K .Jansen, F .Palombi, R .Petronzio, A .Shindler and I. W etzorke [Z euthen-R ome (Z eR o) Collaboration], arX iv:hep-lat/0403009.
- [4] D .A mdt and C .J.D .Lin, arX iv:hep-lat/0403012.
- [5] M .P rocura, T .R .H emmert and W .W eise, Phys. Rev. D 69, 034505 (2004) [arX iv:hep-lat/0309020].
- [6] S.R .B eane and M .J. S avene, arX iv:hep-ph/0404131.
- [7] M .E .B erbenniB itsch, A .D .J ackson, S .M eyer, A .S chafer, J .J .M .V erbaarschot and T .W ettig, Nucl. Phys. Proc. Suppl. 63 (1998) 820 [arX iv:hep-lat/9709102].
- [8] G .C olangelo and C .H aefeli, Phys. Lett. B 590 (2004) 258 [arX iv:hep-lat/0403025].
- [9] G .C olangelo and S .D urr, Eur. Phys. J. C 33 (2004) 543 [arX iv:hep-lat/0311023].
- [10] J .G asser and H .L eutwyler, Phys. Lett. B 184 (1987) 83.
- [11] J .G asser and H .L eutwyler, Phys. Lett. B 188 (1987) 477.
- [12] J .G asser and H .L eutwyler, Nucl. Phys. B 307 (1988) 763.
- [13] H .L eutwyler and A .S milga, Phys. Rev. D 46 (1992) 5607.
- [14] J .G asser and H .L eutwyler, Annals Phys. 158 (1984) 142.
- [15] E .V .S huryak and J .J .M .V erbaarschot, Nucl. Phys. A 560, 306 (1993) [arX iv:hep-th/9212088].
- [16] J .J .M .V erbaarschot, Phys. Rev. Lett. 72, 2531 (1994) [arX iv:hep-th/9401059].
- [17] J .J .M .V erbaarschot, Phys. Lett. B 368, 137 (1996) [arX iv:hep-ph/9509369].
- [18] P .H .D amgaard, R .G .E dwards, U .M .H eller and R .N arayanan, Nucl. Phys. Proc. Suppl. 83, 434 (2000) [arX iv:hep-lat/9909009].
- [19] P .H .D amgaard, R .G .E dwards, U .M .H eller and R .N arayanan, Phys. Rev. D 61, 094503 (2000) [arX iv:hep-lat/9907016].
- [20] M .E .B erbenniB itsch, S .M eyer, A .S chafer, J .J .M .V erbaarschot and T .W ettig, Phys. Rev. Lett. 80, 1146 (1998) [arX iv:hep-lat/9704018].

[21] P. H. Damgaard, U. M. Heller and A. Krasnitz, *Phys. Lett. B* **445**, 366 (1999) [[arX iv:hep-lat/9810060](#)].

[22] B. J. Schaefer and H. J. Pirner, *Nucl. Phys. A* **660** (1999) 439 [[arX iv:nucl-th/9903003](#)].

[23] J. Meyer, K. Schwenzer, H. J. Pirner and A. Deandrea, *Phys. Lett. B* **526**, 79 (2002) [[arX iv:hep-ph/0110279](#)].

[24] G. Papp, B. J. Schaefer, H. J. Pirner and J. Wambach, *Phys. Rev. D* **61**, 096002 (2000) [[arX iv:hep-ph/9909246](#)].

[25] B. J. Schaefer and J. Wambach, [arX iv:nucl-th/0403039](#).

[26] D. U. Jungnickel and C. Wetterich, *Eur. Phys. J. C* **2**, 557 (1998) [[arX iv:hep-ph/9704345](#)].

[27] L. Jendges, K. Schwenzer and H. J. Pirner, *in preparation*.

[28] M. Lüscher, *Commun. Math. Phys.* **104** (1986) 177.

[29] D. U. Jungnickel and C. Wetterich, *Phys. Rev. D* **53** (1996) 5142 [[arX iv:hep-ph/9505267](#)].

[30] J. Berges, D. U. Jungnickel and C. Wetterich, *Phys. Rev. D* **59**, 034010 (1999) [[arX iv:hep-ph/9705474](#)].

[31] J. Meyer, G. Papp, H. J. Pirner and T. Kunihiro, *Phys. Rev. C* **61** (2000) 035202 [[arX iv:nucl-th/9908019](#)].

[32] J. Braun, K. Schwenzer and H. J. Pirner, [arX iv:hep-ph/0312277](#).

[33] J. Zinn-Justin, *Quantum Field Theory And Critical Phenomena*, Oxford, UK : Clarendon (1989), International series of monographs on physics, vol. 77.